Effects of Discrete and Finite Sampling in PatLoc Imaging

G. Schultz[1], M. Zaitsev[1], and J. Hennig[1]
[1]Dept. of Diagnostic Radiology, Medical Physics, University Hospital Freiburg, Freiburg, Germany

Introduction: MRI is characterized by discrete and finite sampling patterns. In Fourier imaging this leads to the well-known truncation artifacts including ringing and also aliasing, if the signal is undersampled. In PatLoc imaging [1] the linear gradient fields are replaced by nonlinear and non-bijective encoding fields. In this case no trivial mapping from frequency space to image space exists. Non-bijective encoding leads to ambiguities, which can be resolved by a suitable parallel imaging reconstruction method. For Cartesian sampling the reconstruction can be performed as described in [2]. However, it is not obvious, how the truncation artifacts appear in PatLoc-reconstructed images. We focus here on quadratic multipolar encoding fields as shown in Fig. 1a,c. These fields cause very good resolution at the periphery of the imaged region, so it is e.g. in particular well suited for cortical imaging. Note that the framework developed in this work is applicable to all sorts of encoding fields.

Basic PatLoc Theory: Consider a parallel imaging setup, in which the PatLoc coils are used instead of the gradients. The signals may be acquired on a regular grid. The signal s^α of receiver coil α with sensitivity profile c^α at k-space location $\vec{k}$ is then given by:

$$s^\alpha(\vec{k}) = \int_V c^\alpha(\vec{x})\rho(\vec{x})e^{i\vec{k}\vec{\omega}(\vec{x})}d\vec{x} = \int_{\omega(V)} \eta^\alpha(\vec{\omega})e^{i\vec{k}\vec{\omega}}d\vec{\omega} \quad \text{with} \quad \eta^\alpha(\vec{\omega}) = \sum_i c_i^\alpha(\vec{\omega})\rho_i(\vec{\omega})d_i(\vec{\omega}) \qquad (1)$$

$\vec{\omega}(\vec{x})$ induces a transformation from image space to frequency space. In 2D-imaging this mapping is defined by two encoding fields (e.g. Fig. 1a,c): $\vec{\omega}(\vec{x}) \propto (B_1(\vec{x}) \quad B_2(\vec{x}))^T$. The factor d_i is a volumetric correction, which comes along with the transformation. The index i indicates that η^α is given by the sum of all identically encoded spins (see e.g. pixel groups in Fig. 1b).

Methods: The theoretical considerations are substantiated by simulations performed in MATLAB (The Mathworks, USA). Sensitivity maps were acquired in a phantom measurement using linear gradient fields. A phase-modulated Shepp-Logan head phantom was used to represent the spin density. Undersampling has been simulated by deleting every second k-space line.

Results and Discussion: Eq. 1 shows that s^α and η^α form a Fourier transform pair. This means that η^α behaves like an image does in Fourier imaging: Discrete and finite sampling leads to the usual ringing (Fig. 2a) and aliasing (Fig. 3d) artifacts as long as η^α is displayed in frequency space. Eq. 1 shows that the magnetization $\rho_i(\vec{\omega})$ can be found correctly by solving a matrix equation. This is true in the discretized case, if the sensitivity profiles and the correction factor d_i are smooth in frequency space. Then $\rho_i(\vec{\omega})$ basically shows the same ringing (Fig. 2b) and aliasing artifacts as $\eta^\alpha(\vec{\omega})$ .The actual image is found by a variable transformation from frequency space to image space: $\tilde{\rho}(\vec{x}) = \rho_i(\vec{\omega})$ evaluated at $\vec{x} = \omega_i^{-1}(\vec{\omega})$. The transformation induces non-symmetric distortions in the point spread function (PSF) and it leads to differences in the distances of aliased pixels.

The comparison of Fig. 2c with Fig. 1b demonstrates that the ringing mainly affects neighbouring pixels, which lie on contour lines of the encoding fields in image space. The shape of these lines only depends on the applied encoding fields, and so the ringing remains interpretable in PatLoc imaging. It should however be noted that the ringing becomes more pronounced and therefore delocalizes in regions, where the encoding fields become flat as signal accumulates in narrow frequency bands. As imaging is not possible in such flat regions anyway, the unwanted artifacts can be suppressed, e.g. by filtering or by adding a linear gradient for intra-voxel dephasing.

Fig. 3b,d depict the aliasing artifacts, if the signal is undersampled. The Nyquist theorem shows that for Cartesian sampling the 2D-FOV is a rectangle in frequency space. In image space a rectangle has a different shape (→ Fig. 3a,b). As long as the object lies within this shape, no aliasing occurs. If the Nyquist-boundary is chosen to be narrower in frequency space, aliasing occurs (→ Fig. 3b,d).

The aliasing can be undone by combining PatLoc reconstruction with SENSE reconstruction [3]. Both reconstruction methods rely on the fact that spins at different, but known positions are identically encoded by the encoding functions, but differently weighted by the sensitivity profiles of the receiver coils. Undersampling with reduction factor R and with an intrinsic PatLoc acceleration of S leads to R*S identically encoded spins. Once the corresponding positions are found, an adequate matrix inversion leads to the desired recovery of the original spin density, if the number of coils exceeds R*S and as long as the g-factor penalty is not severe. An example for R = 2 (and S = 2 for the quadratic multipolar encoding fields) is shown in Fig. 4, which should be seen in conjunction with Fig. 3.

Though the truncation artifacts might appear differently in PatLoc imaging, they can be interpreted easily by differing clearly between image space and frequency space. Understanding the truncation artifacts in PatLoc imaging is important for correct identification of artifacts in images. It also helps to solve a lot of interesting application problems. One application has been shown in this work: The combination of PatLoc reconstruction with SENSE reconstruction.

Acknowledgements: This work is part of the INUMAC project supported by the German Federal Ministry of Education and Research, grant #13N9208.

References: [1] Hennig et al., MAGMA 21(1-2):5 – 14 (2008); [2] Schultz et al., Proc. ISMRM, #786, Toronto (2008); [3] Pruessmann et al., MRM 42, 952 – 962 (1999).

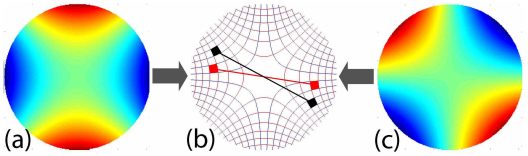

Figure 1: (a) and (c): Multipolar PatLoc-encoding fields. (b) Achievable resolution. The pigmented pixels are examples of pixel groups.

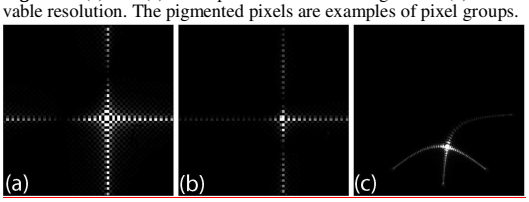

Figure 2: Real parts of PSF weighted with intensity correction showing the ringing artifact. (a) DFT of signal (η^α). (b) PSF in frequency space.after reconstruction (c) Corresponding PSF in image space. Contributing pixels lie on contour lines of the encoding fields (cp. Fig. 1b). The images are overscaled to visualize the artifacts.

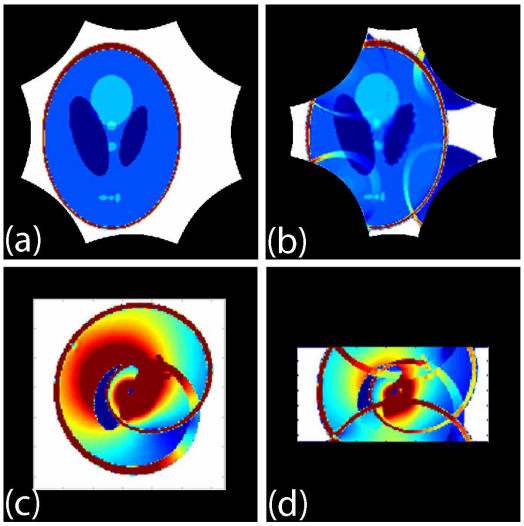

Figure 3: Illustration of the aliasing artifact. (a) and (b): Image space representation; (c) and (d): Frequency space representation. Images (b) and (d) result upon undersampling by factor two. The white areas show the chosen FOVs. The encoding fields define shape and size of the FOVs in image space. The non-unique mapping to image space leads to a 4-fold appearance of the aliasing artifact in image space.

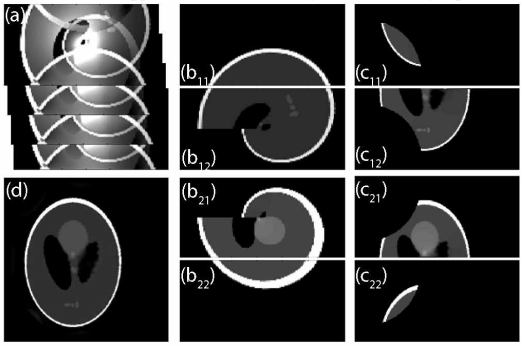

Figure 4: PatLoc reconstructon in combination with two-fold undersampling. (a) DFT of individual coil data. Only four of eight datasets are shown. Aliased pixels are unfolded by reconstruction resulting in (b): Spin density in frequency space. Four realizations of this space exist: the first index indicates realizations induced by the inverse mapping of the encoding fields, the second index indicates the space separation due to undersampling. (c) Respective spin densities in image space. (d) Final image.